Task-based Control of a Multirotor Miniature Aerial Vehicle Having an Onboard Manipulator

J. ESCARENO*, G. FLORES, M. RAKOTONDRABE, H. Romero, R LOZANO and E. RUBIO

***Abstract*— The paper presents the modeling and control of a class of multirotor miniature aerial vehicle (MAV) having an onboard robotic manipulator. These kind of configuration represents the logical evolution in the MAV development race. The main goal is to outstrip the current operational profile, specially in the civilian field, by endowing classical MAV configurations with novel capabilities to interact with the surrounding environment. The equations that describes the dynamic model of this class of aerial robot, for translation and rotational motion, are obtained through the Euler-Lagrange formalism. This energy-based modeling approach allows to obtain the mechanical couplings between both aerial and manipulation systems, the aerial and manipulation. In terms of control, our main goal is to provide a simple-to-implement controller to perform aerial manipulation tasks using multirotor MAVs. A task-based control strategy is then proposed to cancel the couplings in the overall dynamic model (model simplification). The control law for the aerial system relies on a classical two-level scheme to fullfil tracking problem. On the other hand, the motion problem of the manipulation system is addressed via a switching-based controller. The controller corresponding stability proofs are presented and the performance of the control strategy is evaluated at simulation level.**

I. INTRODUCTION

The pace of development of Unmanned Aerial Vehicles (UAVs) has increased over the last few years, due to the wide range of military or civilian applications were they could potentially be deployed. In the military field, applications such as delivering survival-kits to the troops, mobile communication link with a ground station for information exchange, risk evaluation of hostile area, are just a few examples of drone-based applications. It is well know that growth rate of MAVs civilian application is not as high as that of its military counterpart. However, the operational profile offered by interactive MAVs unveils interesting novel applications, for instance, recovering mineral samplings in volcanic study, air-quality cartography/monitoring, placing/recovering sensors in constrained strategic areas, recovering potential explosive packages in sensitive facilities. The interactive MAV configuration represent a unique profile endowing manipulator robot with the 3D mobility of aerial vehicles. The latter allows to perform teleoperated/autonomous interactivity within hostile environments. Whereas this concept is very promising, it also comes with significant robotic and automation challenges. Foremost amongst these is the modeling the compound mechanical system and designing controllers that will work, in theory and practice, over partial or complete operational scope of the flying robot and an appropriate and optimized mechanical design to meet the desired flight performance requirements.

Recent research activities related to interactive flying rotorcrafts can be found in the literature: [2]where the authors have presented the planar model and attitude control analysis of helicopter equipped with a gripper that is capable of grasping and transporting loads of different geometries and sizes. GRASP Research team uses different cooperative quadrotors fleet configurations to transport corresponding load geometries by means of gripper and cables [3]. An alternative UAV configuration featuring a hook aiming at vision-based delivering and retrieving of cargo, is presented in [4]. In [5] and [6], the problem of load transportation using autonomous small size helicopters is addressed. Likewise, the modeling and control of a variable number of helicopters transporting a load is presented. Indeed, the proposed controller prevent and compensate load oscillations during flight, which is demonstrated by real flight load transportation by three helicopters.

The paper presents the study of a class of a multirotor MAV evolving in the longitudinal plane and capable of interacting with the surrounding environment by means of an onboard 1-DOF manipulator. The paper addresses the energy-based modeling and control strategy based on a predefined operational profile (task-based control). From the mechanical point of view, the actual aerial configuration is considered as a multi-body mechanical system, encompassing the aerial (MAV) and manipulation (robot manipulator) systems. Such robotic arm is intended to perform simple prehension tasks, i.e. pick-and-place of simple-geometry objects into/from obstructed cavities. It is clear that in-flight manipulator operations shifts the rotorcraft center of gravity (cg), this is equivalent to having disturbing torques in the nominal rotational dynamics of the rotorcraft. For this reason, the equations of motion based on the Euler-Lagrange formulation are considered for defining the dynamic model of the interactive aerial robot, since it allows to obtain not only the main forces and moments exerted on the vehicle but also the couplings [7][8]. Likewise, we design the controller for the interactive aerial robot a function of two tasks aerial (i) transportation and (2) manipulation, such

J. Escareno is with the Polytechnic Institute of Advanced Sciences, 7-9 rue M. Grandcoing, 94200 Ivry-sur-Seine, France

G. Flores and R. Lozano are with the Heudiasyc Laboratory UMR 7253, Université de Technologie de Compiegne, 60205 Compiegne - France

M. Rakotondrabe is with the FEMTO-ST Institute, UMR CNRS - UFC / ENSMM / UTBM, Automatic Control and Micro-Mechatronic Deparment, 24, rue Alain Savary, Besancon, France

H. Romero is with the ICBI - Universidad Autonoma del Estado de Hidalgo

E. Rubio is with the Laboratorio de Robotica y Mecatronica del Centro de Investigacion de Computo IPN

*Corresponding author: escareno@ipsa.fr

approach is meant to simplify the overall dynamic model and thus the control law synthesis. Since we have defined a specific operational profile, it provides an *a priori* idea of the vehicle's dynamic behavior during each operational mode allowing to eliminate and/or neglect associated couplings, while remaining couplings are considered as disturbances a thus addressed via a robust control scheme.

The outline of the paper is as follows: section II describing the problem arising from having a robotic arm onboard of an miniature vehicle, as well as, is described the translational and rotational mathematical model of the multi-body aerial system. The proposed strategy based on two operational regimes is described in section IV. Numerical simulations results are presented in section V. Conclusions and perspectives are finally given in Section VI.

II. Dynamic Model

This section presents the energy-based equations of motion representing the dynamic behavior of the interactive air robot while evolving within the longitudinal plane (planar model), such equations were obtained via the Euler-Lagrange formulation [10]. Such modeling formalism is useful to obtain dynamic relationships for coupled mechanical configurations (multi-body vehicle). In [10] we have considered a generalized rotational model encompassing rotational dynamics of the rotorcraft and manipulator on a single vectorial expression, however, in the present paper we split the equations of motions in two equations sets for aerial and manipulation systems, respectively. The resulting model is useful to identify inherent dynamic couplings in the overall system, which allows to qualify the influence of such terms aiming at simplifications in the control design. The aerial robot has onboard an actuated robotic manipulator, equipped with a simple (open/close) gripper, carrying a cargo, and hence, its evolution implies additional forces and moments acting on the aerial robot and on the manipulator as well (Fig. 2). According to figure (Fig. 2), θ is the pitch angle, γ is the the manipulator's angle with respect to (w.r.t.) $-e_3$, while $T_1$and T_2 are the thrust provided by frontal and rear rotors, respectively.

A. Kinematics

The kinematics of the flying robot comprise two right-handed reference coordinates systems [9].

- Let (e_x, e_y, e_z) defines the fixed inertial coordinates system $\mathcal{F}^i$, whose origin O^i located at the earth surface. For the longitudinal case the vector basis becomes $(e_x, 0, e_z)$
- Let (e_1, e_2, e_3) be the body-fixed frame $\mathcal{F}^b$, whose origin O^b corresponds to the center of gravity CG of the quadrotor. For the longitudinal case the vector basis becomes (e_1, e_3).
- Figure 2 depicts the vehicle rotating clockwise (righthanded sense) while the manipulator does in the opposite sense. This rotational displacement is expressed by the orthogonal transformation matrices $\mathcal{R}^\theta \in \Re^{2\times 2}$ and $\mathcal{R}^\gamma \in \Re^{2\times 2}$, where θ and γ correspond to the quad-rotor's attitude and manipulator's joint angle, respectively.

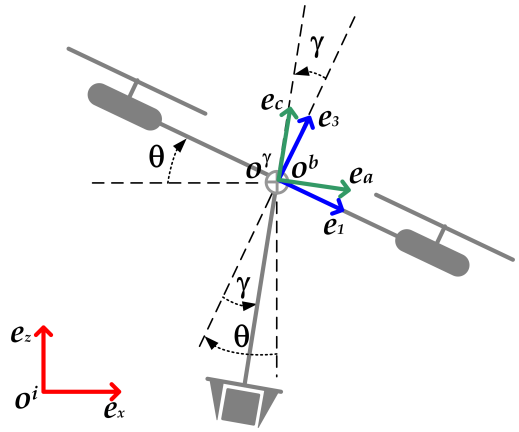

Fig. 1. Frames of reference

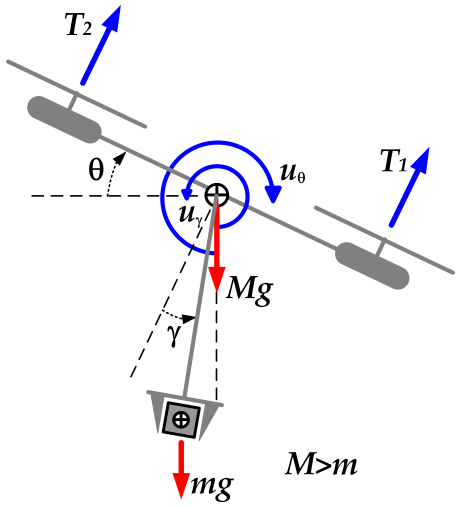

Fig. 2. Forces and moments

B. Equations of motion

The equations of motions of the complete system rotorcraft-manipulator are obtained via the Euler-Lagrange formulation, for details see ([10]).

$$\begin{cases} u_x &= (M+m)\ddot{x} - m\ell\cos(\theta-\gamma)(\ddot{\theta}-\ddot{\gamma}) \\ & \quad +m\ell\sin(\theta-\gamma)(\dot{\theta}-\dot{\gamma})^2 \\ u_z &= (M+m)\ddot{z} + m\ell\sin(\theta-\gamma)(\ddot{\theta}-\ddot{\gamma}) \\ & \quad +m\ell\cos(\theta-\gamma)(\dot{\theta}-\dot{\gamma})^2 + (M+m)g \end{cases} \tag{1}$$

notice that for the translational equation, displacement along the $x-$axis is underactuated by the attitude, i.e. $u_x = 0$. The corresponding equations describing the rotational motion are

$$\begin{cases} u_\theta &= (I_Y + m\ell^2 + I_y)\ddot{\theta} - (m\ell^2 + I_y)\ddot{\gamma} \\ & \quad -m\ell\cos(\theta-\gamma)\ddot{x} + m\ell\sin(\theta-\gamma)\ddot{z} \\ & \quad +mg\ell\sin(\theta-\gamma) \\ u_\gamma &= (I_y + m\ell^2)\ddot{\gamma} - (ml^2 + I_y)\ddot{\theta} + m\ell\cos(\theta-\gamma)\ddot{x} \\ & \quad -m\ell\sin(\theta-\gamma)\ddot{z} - mg\ell\sin(\theta-\gamma) \end{cases} \tag{2}$$

Let us re-group the previous set of equations with respect to the (*i*) aerial and (*ii*) manipulation subsystems

C. Rotorcraft MAV

The equations modeling the translational and rotational aerial system are written

$$\Sigma_A : \begin{cases} (M+m)\ddot{\xi} = \mathbf{U}_\xi + \mathbf{W}_{(\mathbf{M+m})} + \mathbf{F_c} + \mathbf{F_t} \\ I_Y\ddot{\theta} = U_\theta + T_{\theta_t} + T_{\theta_w} + T_{\theta_\xi} \end{cases} \tag{3}$$

where $\dot{\xi} = (\dot{x}, \dot{z})^T$ represents the 2D velocity of the drone, $\mathbf{U}_\xi = \mathcal{R}^\theta \mathbf{F}^b$ the thrust vector used as control input, $\mathbf{W}_{(\mathbf{M+m})} = (0, -(M+m)g)^T$ is the total weight vector, while

$$\begin{aligned} \mathbf{F_c} &= \begin{pmatrix} m\ell\sin(\theta-\gamma)(\dot{\theta}-\dot{\gamma})^2 \\ m\ell\cos(\theta-\gamma)(\dot{\theta}-\dot{\gamma})^2 \end{pmatrix} \\ \mathbf{F_t} &= \begin{pmatrix} m\ell\cos(\theta-\gamma)(\ddot{\theta}-\ddot{\gamma}) \\ -m\ell\sin(\theta-\gamma)(\ddot{\theta}-\ddot{\gamma}) \end{pmatrix} \end{aligned} \tag{4}$$

correspond to the centripetal and tangential forces arising from the rotational motion of the manipulator robot. Concerning the rotational dynamics of aerial system, the following disturbing torques are identified,

$$\begin{aligned} T_{\theta_\xi} &= m\ell\cos(\theta-\gamma)\ddot{x} - m\ell\sin(\theta-\gamma)\ddot{z} \\ T_{\theta_w} &= -mg\ell\sin(\theta-\gamma) \\ T_{\theta_t} &= (m\ell^2 - I_y)(\ddot{\theta}-\ddot{\gamma}) \end{aligned} \tag{5}$$

where T_{θ_ξ} correspond to the the coupling torque arising from the combination of the MAV's translational motion with manipulator's mass, T_{θ_t} stand for the torque resulting from the manipulator and T_{θ_t}

D. Manipulator Robot

The dynamic equation corresponding to the manipulator system are given as

$$\Sigma_M : (I_y + m\ell^2)(\ddot{\gamma} - \ddot{\theta}) = U_\gamma + T_{\gamma_w} + T_{\gamma_\xi} \tag{6}$$

it is observed that the manipulator's dynamics is disturbed by the following torques

$$\begin{aligned} T_{\gamma_w} &= mg\ell\sin(\theta-\gamma) \\ T_{\gamma_\xi} &= -m\ell\cos(\theta-\gamma)\ddot{x} + m\ell\sin(\theta-\gamma)\ddot{z} \end{aligned} \tag{7}$$

where T_{γ_w} denotes the torque arising from the weight of the manipulator while torque T_{γ_ξ} results from the coupling with translational motion of the MAV.

III. Task-based Dynamics

Based on the dynamic models described by (Eqn 3) and (Eqn 6) described above, it defines an operational profile intended to simplify the control design of the flying robot featuring a robotic manipulator. Hence, in order to achieve such objective, the overall operational task of the multi-body rotorcraft is partitioned into two regimes: *transportation task* and *manipulation task* (see Fig. 3).

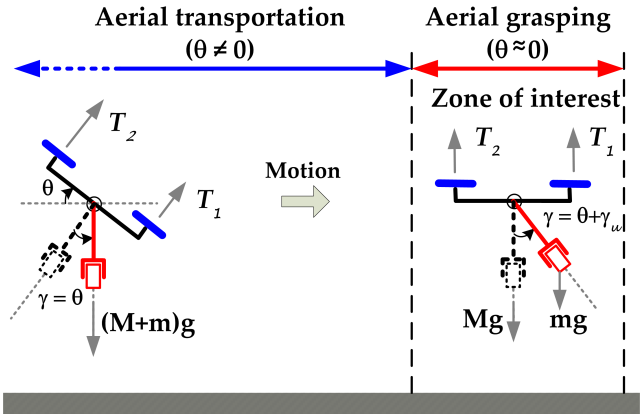

Fig. 3. Overall operational profile of the iMAV showing the location/transportation and manipulation phases.

A. Transportation Task

In order to reduce the coupling during translational operation towards a target zone (manipulation regime), we propose that the manipulator dynamics tracks the state trajectories defined by the attitude of the flying robot, i.e. $\gamma^d = \theta$ and $\dot{\gamma}^d = \dot{\theta}$. Assuming an effective tracking control implies that $T_{\gamma_w} \to 0$ and $T_{\gamma_\xi} \to m\ell\ddot{x}$. Hence, Eqn 6 becomes

$$\Sigma_{M_{trans}} : (I_y + m\ell^2)(\ddot{\gamma} - \ddot{\theta}) = U_\gamma - ml\ddot{x} \tag{8}$$

Achieving such tracking objective (Eqn 8) results in the vertical position of manipulator for any attitude of the rotorcraft, simplifying the dynamic model of the aerial system (Eqn 3) as

$$\Sigma_{A_{trans}} : \begin{cases} (M+m)\ddot{\xi} = \mathbf{U}_\xi + \mathbf{W}_{(M+m)} \\ I_Y\ddot{\theta} = U_\theta + ml\ddot{x} \end{cases} \tag{9}$$

where parasitic forces were neglected, since $\mathbf{F_c} \to (0,0)^T$ and $\mathbf{F_t} \to (\approx 0, 0)^T$.

B. Manipulation Task

Given that the manipulator is meant to evolve for different reference positions (placing/recovering target objects) within this regime, and, the rotorcraft has reached the target zone (i.e. $x \approx x^d, z \approx z^d$) near-hovering flight can be assumed (i.e. $\theta \approx 0$ and $\dot{\theta} \approx 0$). Such operational profile leads to $T_{\gamma_{\gamma_w}} \to \tau_w$ and $T_{\gamma_\xi} \to 0$, allowing to rewrite the manipulator models as

$$\Sigma_{M_{manip}} : (I_y + m\ell^2)(\ddot{\gamma} - \ddot{\theta}) = U_\gamma + \tau_{\gamma_w} \tag{10}$$

where τ_{γ_w} is a slow-time varying value assuming small fluctuations of manipulator's angular velocity.

On the other hand, the rotorcraft dynamics (Eqn 3) is reduced to

$$\Sigma_{A_{manip}} : \begin{cases} (M+m)\ddot{\xi} = \mathbf{U}_\xi + \mathbf{W}_{(M+m)} \\ I_Y\ddot{\theta} = U_\theta + T_{\theta_w} \end{cases} \tag{11}$$

where $T_{\theta_\xi} = 0$ due to the MAV is in hovering flight, and, the remaining disturbing terms arising during the transient $\gamma \to \gamma^d$ are considered as parasitic forces and torques, and thus neglected for the control design (but included in the numerical simulation).

IV. Control Design

A. Rotorcraft: Robust Two-time Scale Control

In this section we present a hierarchical control scheme considering the well-known time-scale separation between rotational and translational dynamics [11]. The main goal is to drive the rotorcraft drone according to the commanded reference while rejecting coupling disturbances provided by the evolution of the onboard manipulator. Based on the operation profile described by (Eqn 9) and (Eqn 11), we are able to use a model for the overall aerial transportation/manipulation task

$$\Sigma_A : \begin{cases} (M+m)\ddot{\xi} = \mathbf{U}_\xi + \mathbf{W}_{(M+m)} \\ I_Y \ddot{\theta} = U_\theta + \delta_\theta \end{cases} \tag{12}$$

where $\delta_\theta = \delta_{trans} + \delta_{manip}$ corresponds to the remaining disturbances arising during each operational task.

1) Outer-loop Control: In order to stabilize the outer-loop we use the control input

$$\mathbf{U}_\xi = (M+m)\left(-K_p\tilde{\xi} - K_v\dot{\tilde{\xi}} + K_i\chi + \ddot{\xi}^d + \mathbf{W}_{(M+m)}\right) \tag{13}$$

where $\tilde{\xi} = \xi - \xi^d$, $\chi = \int \tilde{\xi}$, $K_p = \text{diag}(k_{p_x}, k_{p_z})$, $K_v = \text{diag}(k_{v_x}, k_{v_z})$ and $K_i = \text{diag}(k_{i_x}, k_{i_z})$ correspond to proportional, derivative and integral matrix gains that stabilize the translational error dynamics $\ddot{\tilde{\xi}}$. The magnitude and angle of the control vector (Eqn 13) are the required thrust and attitude to fulfill the trajectory-tracking objective.

2) Inner-loop Control: Unlike the thrust (actual control input) the angle is generated via the pitch dynamics, that is to say, the resulting angle of (Eqn 13) is the commanded reference for the pitch dynamic system. To meet the overall control objective it is necessary to guarantee tracking control of the desired pitch attitude while providing robustness with respect to disturbances encountered within each operational regime.

Let us recall the disturbed dynamic 2nd-order model, which corresponds to the second term of the equation (Eqn 12)

$$I_Y\ddot{\theta} = U_\theta + \delta_\theta \tag{14}$$

which has a pure-feedback (lower-triangular) form suitable to apply the Backstepping method. Since we are concerned in the trajectory tracking problem, we are able to rewrite an extended state-space model in terms of the error variable

$$\begin{array}{rcl} \dot{e}_1 & = & e_2 \\ \dot{e}_2 & = & \frac{1}{I_Y}(u_\theta + \tau_{\gamma_w} + \delta_T) - \ddot{\theta}^d \end{array} \tag{15}$$

where $e_1 = \theta - \theta_d$ and $e_2 = \dot{\theta} - \dot{\theta}_d$ are the position and velocity errors, respectively.

Step 1: Let us propose Lyapunov function to deduce a control that stabilizes the first integrator subsystem (15a)

$$\mathcal{V}_1 = \frac{1}{2}e_1^T e_1 \tag{16}$$

whose time-derivative is give by

$$\dot{\mathcal{V}}_1 = e_1 e_2 \tag{17}$$

which is rendered negative-definite ($\dot{\mathcal{V}}_1(e_0, e_1) < 0$) by using e_2 as virtual controller, i.e. $e_2 = -\lambda_1 e_1$.

Step 2: Let us propose the error variable considering the virtual controller as a reference, i.e. $e_2^d = -\lambda_1 e_1$

$$z = e_2 - e_2^d = e_2 + \lambda_1 e_1 \tag{18}$$

which produces the extended state

$$e_2 = z - \lambda_1 e_1 \tag{19}$$

Computing the time-derivative of Eqn (18) yields

$$\dot{z} = \dot{e}_2 + \lambda_1 \dot{e}_1 \tag{20}$$

where replacing the second term of Eqn (15) and Eqn (19)

$$\dot{z} = \frac{1}{I_Y}(U_\theta + \delta_\theta) - \ddot{\theta}^d + \lambda_1(z - \lambda_1 e_1) \tag{21}$$

The final Lyapunov Function

$$\mathcal{V}_2 = \frac{1}{2}e_1^T e_1 + \frac{1}{2}z^T z \tag{22}$$

whose time-derivative is

$$\dot{\mathcal{V}}_2 = e_1 e_2 + z\dot{z} \tag{23}$$

Substituting (19) and (23) lead us to

$$\dot{\mathcal{V}}_2 = -\lambda_1 e_1^2 + z e_1 + z\left[\frac{1}{I_Y}(U_\theta + \delta_\theta) - \ddot{\theta}^d + \lambda_1(z - \lambda_1 e_1)\right] \tag{24}$$

where we introduce the controller U_θ to render (Eqn 24) into a definite negative Lyapunov function. Notice that the structure of the virtual state (18) can be used as sliding surface, this enable us to include in the controller switching term for disturbance rejection purposes.

$$U_\theta = -\beta\text{sign}(z) + I_Y(\ddot{\theta}^d - \lambda_1(z - \lambda_1 e_1)) - e_1 - \lambda_2 z \tag{25}$$

where $\beta > 0$. Assuming that $|\delta_\theta| < \beta$ the previous controller lead us to

$$\dot{\mathcal{V}}_2 = -\lambda e_1^2 - \lambda_2 z^2 \tag{26}$$

which means that the state vector $\nu = (e_1, z)^T$ converges asymptotically to the origin. If z converge to zero, this means that

$$(e_2 + \lambda_1 e_1) \to 0 \tag{27}$$

which implies that e_2 converges asymptotically to the origin, fulfilling the tracking control objective.

B. Manipulator: Switching-based Control

In order to fulfill the aforementioned operational profile, it is necessary to guarantee the stability of the manipulator controller throughout of both flight profiles. From (Eqn 6), we can write the error dynamics as

$$\ddot{e}_\gamma = \ddot{\gamma} \tag{28}$$

with $e_\gamma = \gamma - \gamma^d$ and $\dot{e}_\gamma = \dot{\gamma} - \dot{\gamma}^d$. In such dynamics, let us assume the slow behavior of $\dot{\gamma}^d$ (i.e. $\ddot{\gamma}^d \approx 0$). In order to chose between two different desired trajectories for

γ according to the operational task, we define the reference signal as

$$\gamma^d = \begin{cases} \theta(t) & if\ |\theta| > \theta_h \\ \gamma_u & if\ |\theta| \leq \theta_h \end{cases} \tag{29}$$

where θ_h represents an arbitrary small pitch value indicating that the target zone is reached, which implies near-hovering flight. The control input U_θ should switch between two different references expressed by (Eqn 29).

From (Eqn 29), when $\gamma^d = \theta(t)$, the closed-loop system may be represented by $\dot{\Gamma} = A_\theta \Gamma$ where $\Gamma = [e_\gamma \ \ \dot{e}_\gamma]^T$ and $A_\theta \in \Re^{2\times 2}$. In the other case, when $\gamma^d = \gamma_u$, the closed-loop system (28) is represented as $\dot{\Gamma} = A_{\gamma_u}\Gamma$, where $A_{\gamma_u} \in \Re^{2\times 2}$.

With the aforementioned considerations, it can be defined a state-dependent switched linear system, given by the closed-loop system together with the switching conditions as

$$\dot{\Gamma} = \begin{cases} A_\theta \Gamma & \text{if} \quad |\Gamma| > \theta_h \\ A_{\gamma_u}\Gamma & \text{if} \quad |\Gamma| \leq \theta_h \end{cases} \tag{30}$$

C. Stability Proof

We can investigate a common Lyapunov function V if the rate of decrease of V along solutions, is not affected by switching. Details on the use of a common Lyapunov function can be found in [12], where the authors have chosen the same pole locations for different subsystems.

In the case of the present application, there are two subsystems for which different controllers are applied, and thus finding a common Lyapunov function in not possible [12]. For this reason, we proceed to investigate multiple Lyapunov functions for each individual subsystem being switched.

To translate the switching boundary to zero, a simple change of coordinates can be made on the bound between the two operational regions. Therefore, without lose of generality, we consider the angle value θ_h, which is the bound between the two operational regions, equal to zero, i.e. $\theta_h = 0$.

It is clear that each individual system in equation (Eqn 30) is stable, since the matrices A_t and A_a are Hurwitz.

Now, we will focus on the system's stability across switching boundaries, i.e., when the desired trajectory changes from θ to γ_a and vice versa. Suppose that there is a family A_p, $p \in \mathcal{P}$ of functions from $\Re^n$ to $\Re^n$, with $\mathcal{P} = 1, 2, ..., m$ defining the finite index set. For the case of linear systems, this results in a family of systems $\dot{x} = A_p x$ with $A_p \in \Re^{n\times n}$. Let's define a piecewise constant function $\sigma : [0, \infty) \to \mathcal{P}$ with finite number of discontinuities (switching times) on every bounded time interval. This function takes a constant value on every interval between two consecutive switching times. Then σ gives the index $\sigma(t) \in \mathcal{P}$ of the system that is actually active, at each instant of time t.

In the particular case presented in this paper, the finite index set is defined as $\mathcal{P} = \{\theta, \gamma_u\}$ and the matrices $A_\theta \in \Re^2$, $A_{\gamma_u} \in \Re^2$ form the linear system (28), (30). Thus, we can establish the following theorem:

Parameter	Value[units]
l	0.35[m]
M	0.4[Kg]
m	0.03 [Kg]
I_Y	0.177 [Kgm^2]
I_y	3.0625×10^{-4}
g	9.8×10^{-4} [Kgm^2]

TABLE I
INTERACTIVE ROTORCRAFT VEHICLE

Theorem 1: Consider vectors t_{pq}, symmetric matrices S_p with $\Omega_p \in \{x : x^T S_p x \geq 0\}$, $\forall p \in \mathcal{P}$ having non-negative entries and symmetric matrices P_p such that:

$$A_p^T P_p + P_p A_p + \beta_p S_p < 0, \qquad \beta_p \geq 0 \tag{31}$$

$$0 < P_p - P_q + f_{pq} t_{pq}^T + t_{pq} f_{pq}^T \text{ for some } t_{pq} \in \Re^n \tag{32}$$

With the boundary between Ω_p and Ω_q of the form $\{x : f_{pq}^T = 0\}$, $f_{pq} \in \Re^n$. Then every continuous, piecewise $\mathcal{C}^1$ trajectory of the system $\dot{x} = A_\sigma x$ tends to zero exponentially.

Proof: [Proof of Theorem 1]

Before proving Theorem 1, let's use the following theorem.

Theorem 2: The system $\dot{x} = f(t, x)$, $f(t, x) \equiv 0$, is exponentially stable on the region $D = \{x \in \Re^n | \|x\| < r\}$ if there exists a Lyapunov function $V(t, x)$ and some positive constants c_1, c_2, c_3, such that $\forall (t, x) \in [0, \infty) \times D_0$, $D_0 = \{x \in \Re^n | \|x\| < r/m\}$

$$c_1 \|x\|^2 \leq V(t, x) \leq c_2 \|x\|^2 \tag{33}$$

$$\frac{\partial V}{\partial t} + \frac{\partial V}{\partial x} \leq -c_3 \|x\|^2 \tag{34}$$

where m is the *overshot* from definition of exponential stability.

Proof: [Proof of Theorem 2]

See [13], pp. 169. ■

The proof of Theorem 1 relies on the Theorem 2, then using the Lyapunov function candidate $V(x) = x^T P_p x$ and assuming that $x(t)$ is continuous and piecewise $\mathcal{C}^1$, hence, $V(t)$ has the same characteristics. Premultiplying and postmultiplying the condition (32) by x, the inequality on the left side of (Eqn 33) is satisfied. In the same way, inequality (Eqn 34) follows if we premultiply and postmultiply both sides of (Eqn 31) by x.

■

V. NUMERICAL SIMULATION

Numerical simulations were carried out in order to support the proposed control strategy evaluating the performance of the rotational and translational disturbed subsystems. In the simulation we use the parameters close to real aerial platforms. Those parameters are depicted in table I

The translational task consisting in reaching $\xi^d = (x^d = 2, z^d = 4)^T$, while the arm is meant to reach a desired angle of $\gamma_d = 20\,\text{deg}$ once on the target zone. The following figures shows the behavior of the flying robot for different values of

switching thresholds θ_h (Eqn 29). We consider the values: (1) $\theta_h = 10deg$, (2) $\theta_h = 5deg$ and (3) $\theta_h = 0.5deg$

1) Significant thresholds generates early activation of the aerial grasping task (Fig.4 Fig.5)
2) It is the required to reduce the threshold to meet the task-based objective (Fig.6 Fig.7)
3) Threshold values near to zero results appropriate to fulfill the control strategy requirements. Since the γ tracks θ during the translational flight (transportation regime) and the manipulator robot reaches the desired reference when the rotorcraft is on the target zone (Fig.8, Fig.9).

In general, the latter results shown that the manipulator robots is capable of the reach different commanded positions, meeting the performance requirements imposed by the task-based strategy. It is also important to highlight that the good performance of rotorcraft's translational states thanks to the robust inner-loop controller (sliding-mode control), which is robust enough to deal with the couplings provided by the manipulation system.

VI. Concluding Remarks and Perspectives

In general the paper presented the modeling and control of a class of rotorcraft featuring an onboard robotic manipulator. The energy-based modeling (Euler-Lagrange formalism) is useful to identify the couplings arising from in kind multi-body air vehicle. Since the full model structure is complex to design a controller, we have proposed an operational profile such that model is simplified. Likewise, the resulting model is then studied in order to apply a robust and switching-based controllers. Specifically, we use a classical hierarchical controller scheme. For the controller synthesis, a classical time-scale separation is assumed between rotational (fast-dynamics inner-loop) and translational motion (slow-dynamics outer loop). Considering that couplings are considered as disturbances in the present study, we use a

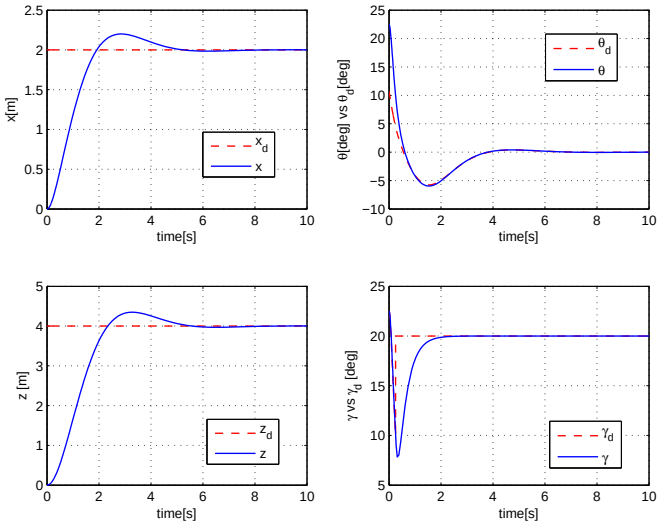

Fig. 4. States evolution: [left] Translational states, [right] Rotational states

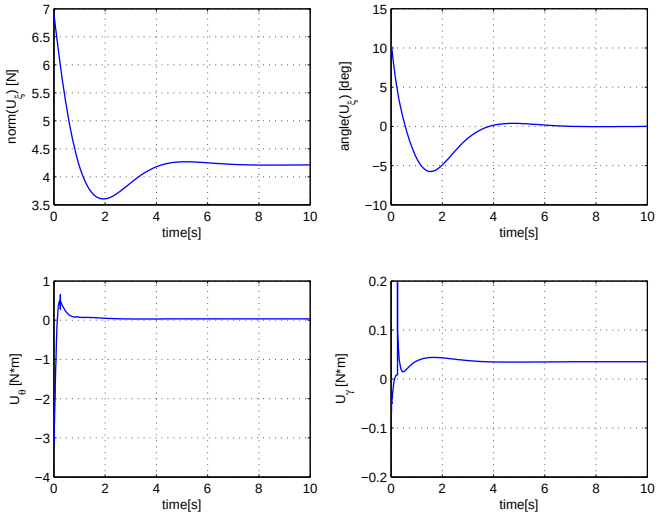

Fig. 5. Control Inputs: [top] Magnitude and Orientation of the translational control vector [bottom] Control inputs for rotorcraft's attitude and manipulator motion

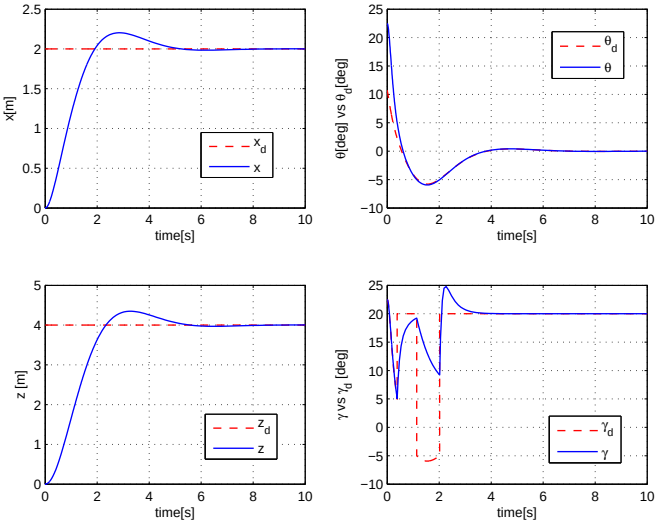

Fig. 6. States evolution: [left] Translational states and [right] rotational states

SMC approach to solve the tracking problem of the inner-loop. Since an task-based operational profile was proposed to mitigate dynamic couplings, a hybrid controller was used to control the manipulator robot throughout the operational scope of the interactive air system. The implementation of such controllers leads to a satisfactorily evolution of the system states fulfilling the control objective. The following stage to be addressed is the extension of this paper to the 3D case considering that the simultaneous operations translation and manipulation.

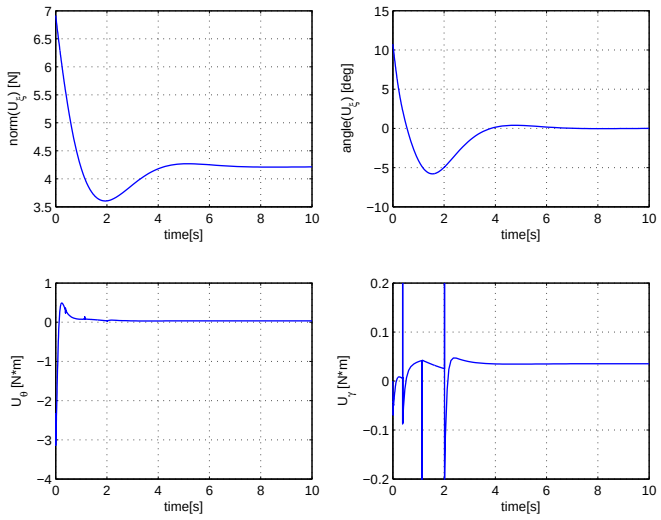

Fig. 7. Control Inputs: [Top] Magnitude and Orientation of the translational control vector [Bottom] Control inputs for rotorcraft's attitude and manipulator motion

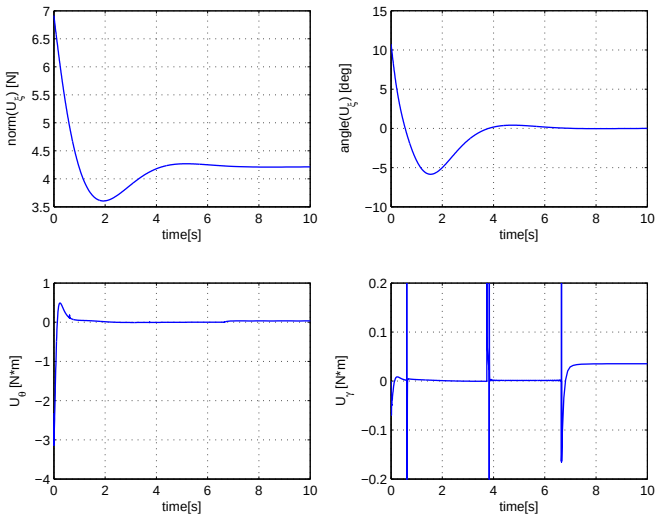

Fig. 9. Control Inputs: [top] Magnitude and Orientation of the translational control vector [bottom] Control inputs for rotorcraft's attitude and manipulator motion

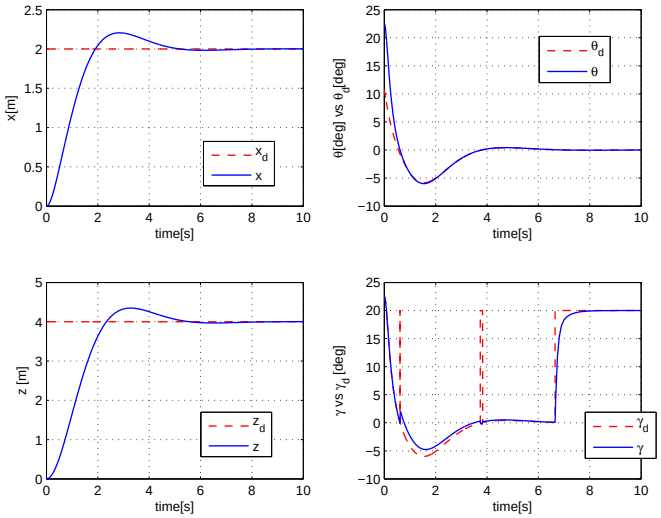

Fig. 8. States evolution: [left:] Translational states, [right:] Rotational states

REFERENCES

[1] Special Issue on Mobile Manipulation, IEEE Robotics and Automation Magazine, June 2012.

[2] Paul E. Pound, Daniel R. Bersak and Aaron M. Dollar, Grasping From the Air: Hovering Capture and Load Stability, *IEEE International Conference on Robotics and Automation*, Shanghai, China, May. 2011.

[3] D. Mellinger, M. Shomin, N. Michael, and V. Kumar, Cooperative Grasping and Transport using Multiple Quadrotors, *Distributed Autonomous Robotic Systems*, Lausanne, Switzerland, Nov 2010

[4] N. Kuntz, P. Y. Oh, Towards Autonomous Cargo Deployment and Retrieval by an Unmanned Aerial Vehicle Using Visual Servoing, in *ASME Dynamic Systems and Controls Conference*, 2008.

[5] M. Bernard, K. Kondak and G. Hommel, Load Transportation System based on Autonomous Small Size Helicopters, *The aeronautical Journal*, March 2010 Vol. 114 No. 1153.

[6] M. Bernard, K. Kondak, I. Maza and A. Ollero, "Autonomous transportation and deployment with aerial robots for search and rescue missions", *Journal of Field Robotics*, vol. 28, No. 6, pp 914-931, 2011.

[7] Goldstein, H., *Classical Mechanics*. Addison-Wesley. ISBN 0201029693 (1980)

[8] Fantoni,I. and Lozano,R.(2002). Nonlinear control for underactuated mechanical systems. In *Communications and control engineering series*, 2002, Springer.

[9] Etkin, B., Reid, L.D.: *Dynamics of Flight*. Wiley, New York. ISBN 0471034185 (1959)

[10] J. Escareno, M. Rakotondrabe, G. Flores, and R. Lozano, "Rotorcraft MAV Having an Onboard Manipulator: Longitudinal Modeling and Robust Control", *European Control Conference*, Zurich, Switzerland, July 17-19 2013.

[11] G. Flores and R. Lozano, "Lyapunov-based controller using singular perturbation theory: An application on a mini-UAV", *American Control Conference*, Washington, D.C., 17-19 June 2013.

[12] D. Liberzon, Switching in Systems and Control. Boston: Birkhuser, 2003.

[13] H. K. Khalil, *Nonlinear Systems*. New York: Prentice Hall, 2002.